

Far-infrared transmission studies on a superconducting $\text{BaPb}_{1-x}\text{Bi}_x\text{O}_3$ thin film: Effects of a carrier scattering rate

C. U. Jung, J. H. Kong, B. H. Park, and T. W. Noh*

Department of Physics and Condensed Matter Research Institute, Seoul National University, Seoul 151-742, Korea

E. J. Choi

Department of Physics, University of Seoul, Seoul 130-743, Korea

(Received 29 September 1998; revised manuscript received 4 December 1998)

We measured transmission spectra of a $\text{BaPb}_{1-x}\text{Bi}_x\text{O}_3$ ($x \sim 0.25$) thin film in the frequency region between 5 and 130 cm^{-1} . At low temperature, there is a BCS-like peak in the transmission spectrum near 21 cm^{-1} , corresponding to $2\Delta(0)/k_B T_c = 3.2 \pm 0.3$, and a suppression at lower frequencies. The transmission measurement in superconducting state covering the frequency region up to 13Δ was found to be useful in probing the scattering rate of carriers. The value of scattering rate, $1/\tau$, was estimated to be about 280 cm^{-1} . This suggests that $\text{BaPb}_{1-x}\text{Bi}_x\text{O}_3$ belongs to the moderately dirty regime ($1/\tau \sim 14 \times 2\Delta$) rather than the extremely dirty regime of the Mattis-Bardeen theory. [S0163-1829(99)00613-X]

I. INTRODUCTION

Cubic perovskite bismuthates, including $\text{BaPb}_{1-x}\text{Bi}_x\text{O}_3$ (BPBO) and $\text{Ba}_{1-x}\text{K}_x\text{BiO}_3$ (BKBO), have attracted much attention due to their interesting physical properties.¹⁻⁷ In spite of their three-dimensional structures, these bismuthates have much in common with two-dimensional high-temperature superconductors. They include a high ratio of superconducting transition temperature T_c to density of states at the Fermi level,^{1,8} existence of collective states in their insulating parent materials,¹ and significant spectral weights in the midinfrared (IR) region.¹⁻³ Moreover, due to their structural simplicity and absence of d electrons, it has been believed that understanding on the bismuthates will provide some insights into the superconducting mechanism of the cuprates.

Tunneling, far-IR reflectivity, and far-IR transmission measurements have been used to investigate superconducting energy gap Δ of the bismuthates.^{2-5,9-11} These methods have their own merits and demerits. Tunneling spectroscopy can provide a detailed information on the superconducting condensate, but it usually requires a sample with a high quality junction. Far-IR spectroscopy tools are less sensitive to the surface (or interface) qualities, since they probe an average response in a skin depth region, which is about one micron. Reflectivity measurements can be performed with a bulk sample, but its reflectivity change around T_c is very small (typically less than a few percent). Although transmission measurements require a high quality thin film, its transmission change around T_c is very large (typically more than a hundred percent). Moreover, a transmission spectrum in a superconducting state usually shows a peak near 2Δ , so temperature-dependent optical energy gap, $2\Delta(T)$, can be easily determined.

There have been several far-IR spectroscopic measurements on BKBO,^{2-4,10} and its 2Δ value is rather well established [i.e., $2\Delta(0) = 4.2 \pm 0.3 k_B T_c$]. Compared with BKBO, optical investigations on superconducting states of BPBO are

quite rare. This is probably due to the fact that its $2\Delta(0)$ value is about 20 cm^{-1} , which cannot be easily covered by conventional spectrophotometers. As far as we know, the only far-IR spectroscopic work on the superconducting states of BPBO was done by Schlesinger *et al.*⁵ They measured the reflectivity of polycrystalline BPBO samples, and found that $2\Delta \cong 3.2 k_B T_c$, roughly in agreement with the weak-coupling BCS theory.

We reported optical properties of epitaxial BPBO films which were grown on MgO substrates by pulsed laser deposition.^{6,7} Through reflectivity and transmission measurements in the frequency region of $0.4 \sim 2.7 \text{ eV}$, we found that they have indirect optical gaps.⁷

From doping dependence of the indirect gap, we found that the metal-semiconductor transition in BPBO should be of a band-crossing type. Recently, we were able to build a lamellar grating far-IR spectrophotometer, which can cover the frequency region of $5 \sim 50 \text{ cm}^{-1}$. This new equipment made it possible for us to look into the superconducting states of BPBO. Especially, using a high quality BPBO thin film, we were able to perform transmission measurements on BPBO.

In this paper, we report far-IR transmission spectra of the BPBO thin film. At a low temperature, a peak was found around 21 cm^{-1} , which corresponds to $2\Delta(0)/k_B T_c \cong 3.2$. As temperature increased toward T_c , the peak position moved to a lower frequency with a reduced peak height. It was found that the Mattis-Bardeen (MB) theory,¹² which assumed that scattering rate $1/\tau$ is much larger than 2Δ (i.e., the so-called "extreme dirty limit"), could not explain our transmission spectra. To get a better agreement, we should introduce a finite scattering rate. It was found that the scattering rate of carriers in BPBO should be about 280 cm^{-1} .

II. EXPERIMENTAL

High quality $\text{BaPb}_{0.75}\text{Bi}_{0.25}\text{O}_3$ films were grown on MgO substrates by pulsed laser deposition.⁶ X-ray-diffraction mea-

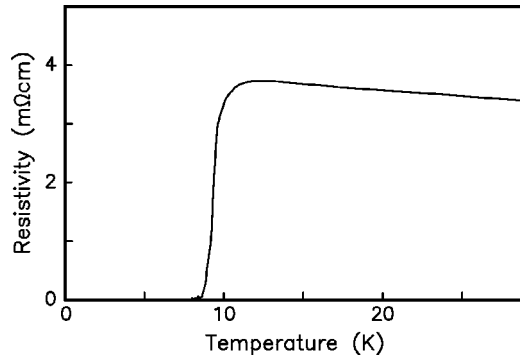


FIG. 1. Resistivity vs. temperature of BPBO thin film.

measurements showed that the films were grown epitaxially with their c axes normal to the substrates. To obtain information on film thicknesses, cross-sectional scanning electron microscope pictures were taken and Rutherford-backscattering spectroscopy (RBS) measurements were performed. The thickness of the $\text{BaPb}_{0.75}\text{Bi}_{0.25}\text{O}_3$ film used in this far-IR study was 570 ± 30 nm. The RBS measurements also showed that the stoichiometry of the film was very close to that of target material.

Figure 1 shows the temperature-dependent resistivity $\rho(T)$ of the $\text{BaPb}_{0.75}\text{Bi}_{0.25}\text{O}_3$ film. The film shows a superconducting transition around 9 K. This T_c value is somewhat lower than the reported value of 12 K for bulk samples.¹ The lower T_c value of the film seemed to originate from thickness effects. Another BPBO film which was about $1.5 \mu\text{m}$ thick had a T_c value of about 11 K. However, this thicker film resulted in a very weak transmission in far-IR region, so it could not be used in our study. Above T_c , $\rho(T)$ seems to decrease slowly with increasing T . This semiconductorlike behavior was observed in bulk BPBO and BKBO samples, indicating that the superconducting transitions are located near the metal-semiconductor transition boundary in the perovskite bismuthates.^{1,13}

Far-IR spectroscopy is known to be quite difficult, since there are no good detectors and light sources in this frequency region. A conventional Michelson-type far-IR spectrophotometer uses a mylar beam splitter, which limits its interferometric modulation efficiency below 0.5. In the dc limit (i.e., $\omega \rightarrow 0$), this efficiency actually approaches zero.¹⁴ Therefore, the Michelson-type spectrophotometer cannot be used to measure spectra in a very low frequency region, typically below 20 cm^{-1} . In order to overcome such difficulties, we recently built a lamellar grating spectrophotometer, whose modulation efficiency was nearly one in the mm wave region.¹⁴ And, we put a Hg arc lamp at one of the focal points in an elliptical mirror, so we could increase the light intensity significantly. With a composite bolometer operating at 1.4 K, we were able to measure far-infrared spectra reliably in the frequency region of $5 \sim 50 \text{ cm}^{-1}$. Details of our new spectrophotometer will be reported elsewhere.¹⁵

The far-IR transmission spectra $\mathcal{T}(\omega)$ of our BPBO film were measured using two kinds of Fourier-transform spectrophotometers. In the frequency region of $5 \sim 35 \text{ cm}^{-1}$, the lamellar grating spectrophotometer, described earlier, was used. In the frequency region of $20 \sim 130 \text{ cm}^{-1}$, a Michelson-type spectrophotometer was used with a Si bo-

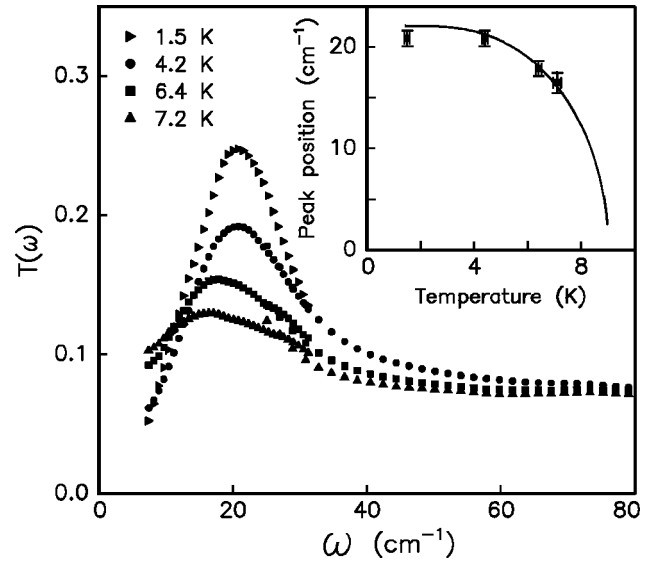


FIG. 2. Transmission spectrum of BPBO thin film at several temperatures below T_c . Peak position moves to a lower frequency as temperature increases. In the inset the symbols represent the peak position of the transmission and the line represents BCS gap function with $2\Delta(0)/k_B T_c = 3.3$. Inset shows that temperature dependence of the peak position is qualitatively consistent with that of BCS gap function.

lometer working at 4.2 K. For most far-IR transmission measurements on a thin film sample, Fabry-Perot interference fringes coming from coherent multiple reflections inside the substrate can cause serious problems.¹⁶ To avoid such difficulties, we used a thick substrate (a thickness of about 2 mm) and performed low resolution measurements. The resolution of our measurements was 1.5 cm^{-1} . With such a low resolution, our experimental spectra did not show any interference fringes. So, our spectra should be understood in terms of incoherent addition of the multiple reflections inside the substrate.

Figure 2 shows $\mathcal{T}(\omega)$ of our BPBO film measured at several temperatures between 1.5 K and T_c . These spectra show characteristics of superconducting thin films, including a peak structure near 21 cm^{-1} and a superfluid screening at the low frequency. [For a typical superconducting film, $\mathcal{T}(\omega)$ approaches zero due to the superfluid screening as ω approaches zero.¹⁷] Note that, in the frequency region of $20 \sim 35 \text{ cm}^{-1}$, the overlaps of $\mathcal{T}(\omega)$ measured by two spectrophotometers are quite good.

III. DATA ANALYSIS AND DISCUSSION

A. A comparison with the Mattis-Bardeen theory

Figure 3 shows $\mathcal{T}(\omega)$ of our BPBO thin film at 4.2 K, where the temperature stability of our measurements was a maximum. The experimental $\mathcal{T}(\omega)$, shown as the solid circles, displayed a peak near 21 cm^{-1} . This peak should be closely related to 2Δ . The low-frequency behavior is dominated by the superfluid screening, which leads to a reduction of transmission below the gap. The prominence of the gap-

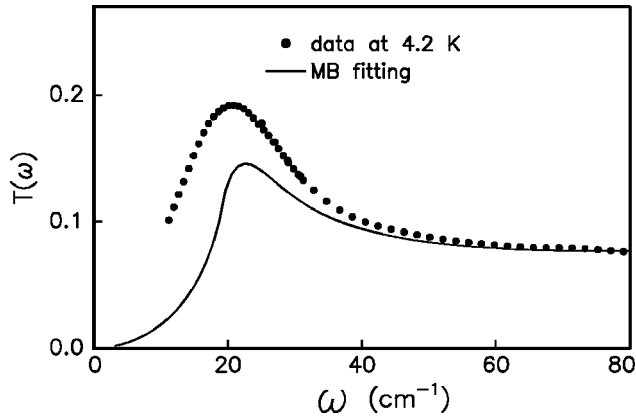


FIG. 3. Transmission spectrum of BPBO thin film at $T = 4.2$ K. The symbols represent the experimental data. The line is calculated with Mattis-Bardeen conductivity with $2\Delta(0)/k_B T_c = 3.2$.

related features implies that its superconducting electrodynamics should be in the dirty limit ($\Delta < 1/\tau$). Note that, in the clean limit ($\Delta > 1/\tau$), the gap-related features should be weak, since there are little oscillator strength changes near 2Δ .¹⁷ Since BPBO seemed to belong to the dirty limit, we decided to compare $\mathcal{T}(\omega)$ with predictions of the MB theory,¹² which explains electrodynamic responses of a BCS-type superconductor in the extremely dirty limit ($\Delta \ll 1/\tau$).

In the thin-film approximation ($\lambda \gg \lambda_p \gg d$, where λ is the radiation wavelength, λ_p is the penetration depth, and d is the film thickness), an approximate form of \mathcal{T} is well known.¹⁶ Taking into account of incoherent addition of the multiple reflections inside the substrate, \mathcal{T} can be approximated as^{4,18}

$$\mathcal{T} = \frac{4n}{|1 + N + y|^2} \left[\frac{\mathcal{T}_s \exp(-\alpha x)}{|1 - \mathcal{R}_s \mathcal{R}_f \exp(-2\alpha x)|} \right], \quad (1)$$

where $N = n + ik$, $\alpha = (4\pi\omega k)$ and x are the complex refractive index, the absorption coefficient, and the thickness of the MgO substrate, respectively. $\mathcal{T}_s = 4n/|1 + N|^2$ and $\mathcal{R}_s = |1 - N|^2/|1 + N|^2$ are the transmission and the reflectivity of the substrate-vacuum boundary, and $\mathcal{R}_f = |N - 1 + y|^2/|N + 1 + y|^2$ is the reflectivity of the substrate-film boundary, with $y = (4\pi\sigma d/c)$, where σ is the frequency-dependent complex ac conductivity of the film.

It was found that the MB theory cannot explain our experimental data. The solid line in Fig. 3 shows the prediction of the MB theory. For this calculation, the optical indices of the MgO substrate were taken from the literature.^{4,19} The normal-state dc conductivity σ_N was $3.5 \times 10^{14} \text{ sec}^{-1}$.²⁰ The $\mathcal{T}(\omega)$ peak is located around 21 cm^{-1} , which corresponds to $2\Delta(0)/k_B T_c \approx 3.2$. Earlier, Schlesinger *et al.* reported that $2\Delta(0)/k_B T_c \approx 3.2$ using far-IR reflectivity measurements,⁵ and Sharifi *et al.* reported that $2\Delta(0)/k_B T_c \approx 3.5 \pm 0.3$ using electron-tunneling measurements.⁹ The value of $2\Delta(0)$ suggests that BPBO should be a weak-coupled BCS superconductor. However, note that the theoretical value of the $\mathcal{T}(\omega)$ peak near the superconducting gap are less than the experimental value by about 20 percent. This difference might be due to a finite scattering rate of carriers inside BPBO, which was neglected in the MB theory.

B. Effects of finite scattering rate

One of important physical quantities in oxide superconductors is the ratio between $1/\tau$ and $2\Delta(0)$. For most metal superconductors, such as Al and Pb, a typical value of $1/\tau$ is about 500 cm^{-1} , so $(1/\tau)/2\Delta(0) \geq 100$. For such BCS superconductors in the extremely dirty limit, their optical responses can be explained by the MB theory. However, in high- T_c superconductors, their $2\Delta(0)$ values are much larger than those of metal superconductors. Although there have been disputes about their electrodynamic responses,²¹ many workers nowadays believe that high- T_c superconductors belong to the clean limit, where $(1/\tau)/2\Delta(0) \leq 1$.²² Inspired by the electrodynamic responses of the high- T_c superconductors, Zimmermann *et al.* investigated effects of a finite scattering rate of carriers on an optical conductivity of a BCS superconductor.²³ They found that optical responses of a superconductor with $(1/\tau)/2\Delta(0) \sim 10$ could be quite different from those with $(1/\tau)/2\Delta(0) \sim 100$, even though both cases belong to the dirty limit. And, such a difference could be seen clearly in the frequency region higher than 2Δ .

To explain the discrepancy of $\mathcal{T}(\omega)$ in Fig. 3, we included the $1/\tau$ effects following the formalism developed by Zimmermann *et al.*²³ Figure 4(a) shows $\mathcal{T}(\omega)$ calculated for three values of the scattering rate, i.e., $1/\tau = 160, 280,$ and 4000 cm^{-1} . In these calculations, $2\Delta(0)$ and σ_N were assumed to be 20 cm^{-1} and $3.5 \times 10^{14} \text{ sec}^{-1}$, respectively. The calculated transmission spectrum for $1/\tau = 4000 \text{ cm}^{-1}$ is almost the same as that of the MB theory (i.e., $1/\tau = \infty$). As $1/\tau$ decreases, the peak height at 2Δ increases and the slope of $\mathcal{T}(\omega)$ above 4Δ also increases. It was also found that the calculated $\mathcal{T}(\omega)$ depends strongly on $1/\tau$ in the regime of $(1/\tau)/2\Delta(0) \sim 10$. Both the peak height and the higher frequency behavior up to $\omega = 130 \text{ cm}^{-1}$ could be fitted reasonably well with $1/\tau = 280 \text{ cm}^{-1}$.

The frequency dependence of $\mathcal{T}(\omega)$ can be understood from optical conductivity, $\sigma(\omega) = \sigma_1(\omega) + i\sigma_2(\omega)$. Figures 4(b) and (c) display $\sigma_1(\omega)/\sigma_N$ and $\sigma_2(\omega)/\sigma_N$, respectively. The dotted and the solid lines represent cases of a normal state (i.e., $T > T_c$) and a superconducting state ($T = 4.2 \text{ K}$) with $1/\tau = 280 \text{ cm}^{-1}$, respectively. In the normal state, $\sigma_1(\omega)$ decreases very slowly up to 130 cm^{-1} , since the corresponding spectral region is lower than $1/\tau$. And, $\sigma_2(\omega)$ increases linearly with ω . In the superconducting state, the spectral weight of $\sigma_1(\omega)$ near 2Δ is reduced, and the decreased amount should move to a zero-frequency delta function, representing a superconducting condensate. (The sharp peak at zero frequency is broadened due to finite temperature.) And, $\sigma_2(\omega)$ becomes inversely proportional to ω at the low frequency. In this region, the divergence of $\sigma_2(\omega)$ makes $\mathcal{T}(\omega)$ in the superconducting state approach to zero as $\omega \rightarrow 0$. From Eq. (1), $\mathcal{T}(\omega) \propto \omega^2$. In the high-frequency region of $\omega \gg 2\Delta$, $\sigma(\omega)$ in the superconducting state approaches to that in the normal state, since a photon with such a high frequency cannot tell the difference in these two states. Therefore, $\mathcal{T}(\omega)$ in the superconducting state is nearly the same as that in the normal state, which is nearly flat in the frequency region of $\omega < 1/\tau$. The peak in $\mathcal{T}(\omega)$ should be located near 2Δ , where $\sigma_1(\omega)$ is nearly zero and $\sigma_2(\omega)$ is drastically decreasing, resulting in a minimum value of absolute magnitude of $\sigma(\omega)$.

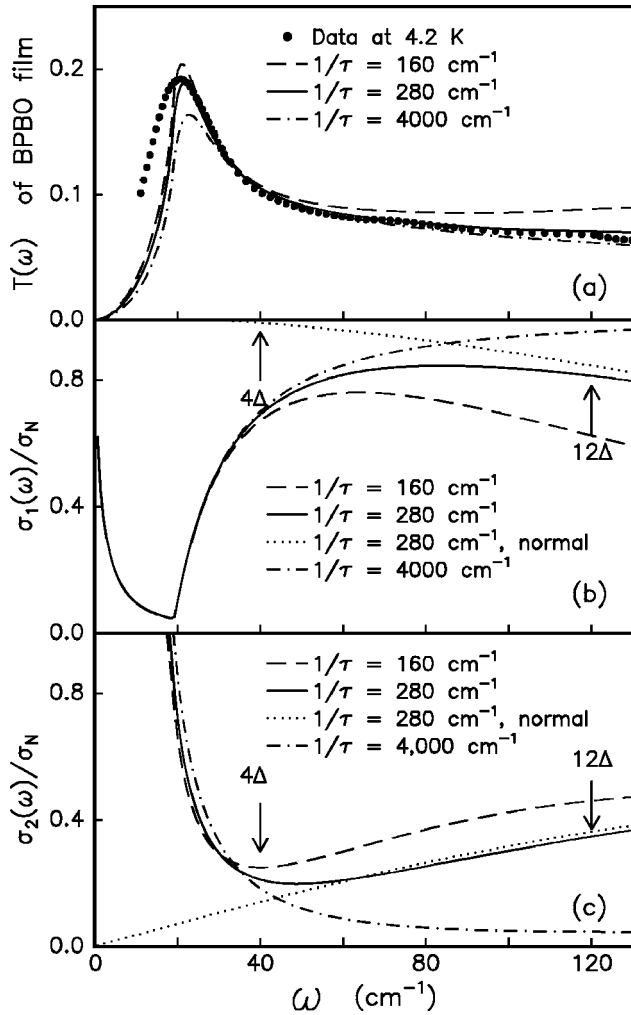


FIG. 4. Calculated transmission of BPBO: moderately dirty limit vs extremely dirty limit. $2\Delta(0)/k_B T_c = 3.2$, $T = 4.2 \text{ K}$, and $T_c = 9.0 \text{ K}$. (a) Transmission data (filled circles) in comparison with the calculated transmission (lines) with ac conductivity with various scattering rate. Best-fit parameters are $1/\tau = 280 \text{ cm}^{-1}$, $\sigma_N = 3.5 \times 10^{14} \text{ sec}^{-1}$. (b) Real part of conductivity in the superconducting state normalized by σ_N . $1/\tau = 160, 280, 4000 \text{ cm}^{-1}$, each corresponding to $1/2\Delta\tau = 8, 14, 200$ with $2\Delta = 20 \text{ cm}^{-1}$. Dotted line represents real part of normal-state Drude conductivity with $1/\tau = 280 \text{ cm}^{-1}$. (c) Imaginary part of conductivity in the superconducting state. Dotted line represents imaginary part of normal-state Drude conductivity with $1/\tau = 280 \text{ cm}^{-1}$.

The scattering rate dependence of $T(\omega)$ can be also understood from the behaviors of $\sigma_1(\omega)$ and $\sigma_2(\omega)$. The dashed, solid, and dashed-dotted lines in Figs. 4(b) and (c) represent the superconducting cases of $1/\tau = 160, 280,$ and 4000 cm^{-1} , respectively. [As we mentioned above, $\sigma_1(\omega)$ and $\sigma_2(\omega)$ of the normal-state will be nearly the same as those of the superconducting state in the frequency region of $\omega \gg 2\Delta$. For clarity, we omitted the normal state responses of $1/\tau = 160$ and 4000 cm^{-1} .] Neglecting the correction factor due to multiple reflections and absorption in the substrate (i.e., the term in the square brackets) from Eq. (1), $T(\omega) \propto 4n/|N+1+y|^2 \propto \alpha y^{-2} \propto \sigma^{-2}$ since $|N| < |y|$ and N is only weakly dependent on ω .¹⁹ Therefore, the behaviors in $T(\omega)$ will depend on the magnitude and the change of $\sigma(\omega)$. Near 2Δ , where the peak in $T(\omega)$ is located, $\sigma_1(\omega) \ll \sigma_2(\omega)$ and

most changes occurs in $\sigma_2(\omega)$. As $1/\tau$ increases, $\sigma_2(\omega)$ increases, resulting in the decrease of the peak height. For the frequency above 4Δ , both $\sigma_1(\omega)$ and $\sigma_2(\omega)$ change. However, since $\sigma_1(\omega) > \sigma_2(\omega)$, the $T(\omega)$ behavior will be dominated by changes in $\sigma_1(\omega)$. As $1/\tau$ increases, $\sigma_1(\omega)$ increases, so $T(\omega)$ decreases.²⁴

As we demonstrated in Fig. 4, measurements of $T(\omega)$ in superconducting films can be useful in determining values of $1/\tau$ quite accurately. Tajima *et al.* measured reflectivity spectra $\mathcal{R}(\omega)$ of $\text{BaPb}_{1-x}\text{Bi}_x\text{O}_3$ for various values of x .¹ Their reflectivity spectra for $x \approx 0.2$ showed a feature similar to a plasma edge around 1 eV . Although there were some deviations of $\mathcal{R}(\omega)$ from the simple free-carrier response, Schlesinger *et al.* assumed the Drude model. Using the relation such that $1/\tau = \omega_D^2/4\pi\sigma_N$, where ω_D is the plasma frequency, they estimated that $1/\tau \sim 8000 \text{ cm}^{-1}$.⁵ Note that this value from the reflectivity measurements is very different from the value of $1/\tau$ ($\sim 280 \text{ cm}^{-1}$) determined from our transmission measurements. The large difference in $1/\tau$ suggests that the interpretation based on the simple Drude model could not be applied for BPBO.

A similar problem in estimating a value of $1/\tau$ can be also found in the BKBO system. Dunmore *et al.* measured transmission spectra of a BKBO film.⁴ Using the simple Drude model, they estimated that $1/\tau \sim 100 \times 2\Delta(0) \sim 4000 \text{ cm}^{-1}$. Later, Puchkov *et al.* measured reflectivity spectra of a BKBO single crystal.^{2,3} Based on the “two-component model,” which assumes coexistence of a sharp Drude peak and a very broad mid-IR peak, they estimated $1/\tau$ for the Drude carrier to be about 250 cm^{-1} .²⁵ And they found that the mean-free-path l for the Drude component and for the mid-IR component will be about 230 and 7 \AA , respectively.

To get more insights on BPBO, we estimated values of electrodynamic parameters for its free carriers. From the earlier specific heat measurements,^{26,27} the effective mass of the carriers was estimated to be about 1.5 times the mass of bare electron (i.e., $m^*/m_e \sim 1.5$). Based on the free-electron model, values of numerous transport quantities were obtained from our experimental values of $\sigma_N \cong 400 \Omega^{-1} \text{ cm}^{-1}$ and $1/\tau \cong 280 \text{ cm}^{-1}$: the average Fermi velocity $v_F \cong 1.2 \times 10^7 \text{ cm/sec}$, the mean free path $l \cong 22 \text{ \AA}$, and the carrier density $n \cong 1.1 \times 10^{20} \text{ cm}^{-3}$. Our estimated value of v_F is smaller by a factor of about 2.5 than other reported values.^{27–29} For the mean free path, we estimated its value from previous transport measurements^{27–29} and found that $l = 6–14 \text{ \AA}$. On the other hand, the scattering rate suggested by IR reflectivity measurement (i.e., $1/\tau = 8000 \text{ cm}^{-1}$)⁵ suggested $l \cong 2 \text{ \AA}$. Clearly, our value of l is somewhat larger than the earlier reported values for BPBO, but smaller than the reported value for BKBO by Puchkov *et al.*

Note that our calculated free-carrier density was about $1.1 \times 10^{20} \text{ cm}^{-3}$, which is one order of magnitude smaller than reported values by Hall measurements.^{28,29} One possibility for this difference can be inferred from the reports that the carrier density of oxygen reduced film can be reduced significantly.^{28,29} However, since we annealed the BPBO film in the oxygen environment, such a possibility will be small. The Hall measurements suggested that metallic free carrier and semiconducting carrier might coexist.^{13,28,29}

Based on the temperature dependence, they suggested that the carrier densities of the free and semiconducting carriers at room temperature might be similar, with $n \sim 1 \times 10^{21} \text{ cm}^{-3}$. And, at low temperature, most of semiconducting carriers were supposed to be suppressed. However, we think that separating the two carrier contributions might be difficult in the Hall measurements.³⁰ Most resistivity measurements on BPBO show that resistivity increases even at low temperature, implying the simple interpretation of the Hall measurement might not be correct. Further investigations are required to clearly understand the electrodynamic responses of BPBO.

In this paper, we analyzed our far-IR data in terms of the simple Drude model. In numerous conducting oxides, including high- T_c superconductors²¹ and colossal magnetoresistance manganites³¹, relatively strong absorption features were observed in the frequency region between far IR and mid IR. There have been three different interpretations: (a) the simple Drude model, (b) the modified Drude model using a frequency dependent scattering rate (called the ‘‘one-component model’’), and (c) the model using a sharp Drude peak and a very broad mid-IR peak (called, the ‘‘two-component model’’). Even though the latter two models are different in their interpretations, it is often quite difficult to distinguish between them experimentally. More accurate measurements, especially using transmission measurements in the far-IR region, would be desirable to determine the electrodynamic responses.

C. Temperature dependence of transmission

From the temperature-dependent $\mathcal{T}(\omega)$, shown in Fig. 2, we could observe several characteristics consistent with BCS predictions. As temperature increases, the peak position shifts to a lower-frequency and the peak height becomes decreased. The low-frequency feature of the superfluid screening, that is the decrease of $\mathcal{T}(\omega)$ as $\omega \rightarrow 0$, becomes weaker. These facts imply that the value of 2Δ decreases and that the suppression of $\sigma_1(\omega)$ due to gap opening becomes weaker. The inset shows that the temperature dependence of 2Δ for the BPBO film agrees with the BCS prediction with $2\Delta(0)/k_B T_c = 3.2$.

Figure 5 shows detailed curve fittings of the experimental $\mathcal{T}(\omega)$ at 4.2 and 7.2 K. The dashed line shows the BCS prediction for 4.2 K with $2\Delta(0) = 20 \text{ cm}^{-1}$, $1/\tau = 280 \text{ cm}^{-1}$, and $\sigma_N = 3.5 \times 10^{14} \text{ sec}^{-1}$. In the frequency region above 20 cm^{-1} , the theoretical curve agrees quite well with the experimental curve. The dotted line shows the BCS prediction for 7.2 K with the above-mentioned parameter values. The theoretical curve above 20 cm^{-1} seems to be a little higher than the experimental data. When we used $\sigma_N = 3.7 \times 10^{14} \text{ sec}^{-1}$ and $1/\tau = 210 \text{ cm}^{-1}$, the theoretical curve, shown as the solid line, provided a better agreement with the experimental data. The new value for σ_N seems to be consistent with the semiconducting behavior in Fig. 1. Note that the change of σ_N by about 5.5% can provide a noticeable change in $\mathcal{T}(\omega)$, demonstrating sensitivity of our transmission measurements.

As shown in Fig. 5, the behavior of experimental $\mathcal{T}(\omega)$ in the frequency region below the peak shows a significant de-

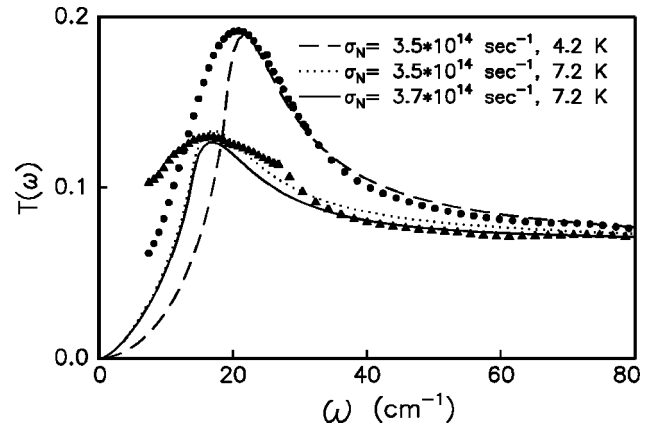


FIG. 5. Fitting of transmission considering the temperature dependence of dc resistivity. Solid circles and triangles represent transmission at 4.2 and 7.2 K. Dashed line and dotted line represent calculated transmission at 4.2 and 7.2 K with same value of σ_N . Solid line represents calculated transmission at 7.2 K with slightly different value of σ_N .

viation from the theoretical curve. This deviation might come from the inhomogeneity of the film: for examples, some part of the film might have a lower T_c value than other part. To take account of such inhomogeneity effects, we assumed a distribution of T_c values and considered three averaging methods: averages of $\sigma(\omega)$,¹⁸ $1/\sigma(\omega)$,³² and $\mathcal{T}(\omega)$. However, it was found that none of such average processes could improve the deviations at the low-frequency region. Further investigations are required to explain the deviations better.

IV. SUMMARY

The experimental data in this paper represent a far-infrared transmission spectra of a superconducting $\text{BaPb}_{0.75}\text{Bi}_{0.25}\text{O}_3$ film. The spectra covered a sufficiently low-frequency region ($\omega \sim 1/2 \times 2\Delta$) to critically test whether this material shows BCS-like behaviors and a high-frequency range ($4\Delta < \omega < 12\Delta$) to reveal that the scattering rate of carriers is not very large. There is a BCS-like peak in the transmission spectrum near 21 cm^{-1} , corresponding to $2\Delta(0)/k_B T_c = 3.2 \pm 0.3$. Detailed shapes of the transmission spectra show deviations from predictions of the MB theory. Calculations in the moderately dirty limit, $1/\tau \sim 14 \times 2\Delta$, gave better results for the peak height and the response above 21 cm^{-1} .

ACKNOWLEDGMENTS

We greatly acknowledge A. J. Sievers, H. J. Lee, and Y. S. Lee, and G. T. Kim for their discussion and help. This work was financially supported by the Ministry of Education through the Basic Science Research Institute Program No. BSRI-97-2416 and by the Korea Science & Engineering Foundation through Grant No. 96-0702-02-01-3 and by the Korea Science & Engineering Foundation through RCDAMP of Pusan National University.

*Electronic address : twnoh@phy.snu.ac.kr

- ¹S. Uchida, K. Kitazawa, and S. Tanaka, *Phase Transit.* **8**, 95 (1987); S. Tajima, S. Uchida, A. Masaki, H. Takagi, K. Kitazawa, S. Tanaka, and A. Katsui, *Phys. Rev. B* **32**, 6302 (1985).
- ²A. V. Puchkov, T. Timusk, W. D. Mosley, and R. N. Shelton, *Phys. Rev. B* **50**, 4144 (1994).
- ³A. V. Puchkov, T. Timusk, M. A. Karlow, S. L. Cooper, P. D. Han, and D. A. Payne, *Phys. Rev. B* **54**, 6686 (1996).
- ⁴F. J. Dunmore, H. D. Drew, E. J. Nicol, E. S. Hellman, and E. H. Hartford, *Phys. Rev. B* **50**, 643 (1994).
- ⁵Z. Schlesinger, R. T. Collins, B. A. Scott, and J. A. Calise, *Phys. Rev. B* **38**, 9284 (1988).
- ⁶Kyoung Ha Kim, C. U. Jung, T. W. Noh, and S. C. Kim, *J. Korean Phys. Soc.* **29**, 515 (1996).
- ⁷Kyoung Ha Kim, C. U. Jung, T. W. Noh, and S. C. Kim, *Phys. Rev. B* **55**, 15 393 (1997).
- ⁸B. Batlogg, in *Mechanisms of High Temperature Superconductivity*, edited by H. Kamimure and A. Oshiyama, Springer Series in Material Science, Vol. 11 (Springer, New York, 1989), p. 342.
- ⁹F. Sharifi, A. Pargellis, R. C. Dynes, B. Miller, E. S. Hellman, J. Rosamilia, and E. H. Hartford, Jr., *Phys. Rev. B* **44**, 12 521 (1991); A. Kussmaul, E. S. Hellman, E. H. Hartford, Jr., and P. M. Tedrow, *Appl. Phys. Lett.* **63**, 2824 (1993).
- ¹⁰Z. Schlesinger, R. T. Collins, J. A. Calise, D. G. Hinks, A. W. Mitchell, Y. Zheng, B. Dabrowski, N. E. Bickers, and D. J. Scalapaino, *Phys. Rev. B* **40**, 6862 (1989).
- ¹¹H. Sato, T. Ido, S. Uchida, S. Tajima, M. Yoshida, K. Tanabe, K. Tatsuhara, and N. Miura, *Phys. Rev. B* **48**, 6617 (1993).
- ¹²D. C. Mattis and J. Bardeen, *Phys. Rev.* **111**, 412 (1958).
- ¹³E. S. Hellman and E. H. Hartford, Jr., *Phys. Rev. B* **47**, 11 346 (1993).
- ¹⁴R. J. Bell, in *Introductory Fourier Transform Spectroscopy* (Academic Press, London, 1972), p. 200.
- ¹⁵C. U. Jung, J. H. Kong, and T. W. Noh (unpublished).
- ¹⁶An explicit and more rigorous way to add the multiple reflection inside the substrate incoherently and to add that inside the film coherently is called the intensity transfer matrix method (ITMM). This method has been effectively applied to optical studies on numerous thin films. [For example, see H. S. Choi, J. S. Ahn, W. Jo, and T. W. Noh, *J. Korean Phys. Soc.* **28**, 636 (1995).] The Eq. (1) was found to provide predictions which are nearly the same as those from the ITMM by varying the dc conductivity value by less than 2%. Due to the simplicity, we used Eq. (1) in our data analysis.
- ¹⁷R. E. Glover and M. Tinkham, *Phys. Rev.* **108**, 243 (1957).
- ¹⁸E.-J. Choi, K. P. Stewart, S. K. Kaplan, H. D. Drew, S. N. Mao, and T. Venkatesan, *Phys. Rev. B* **53**, 8859 (1996).
- ¹⁹T. R. Yang, Sidney Perkowitz, G. L. Carr, R. C. Budhani, G. P. Williams, and C. J. Hirschmugl, *Appl. Opt.* **29**, 332 (1990)
- ²⁰The measured σ_N by four-point probe method was slightly smaller than this value, shown in Fig. 1. This fact represents that bulk σ_N probed by the transmission experiment is not sensitive to grain boundaries in film, contrary to the σ_N value obtained by the transport measurements.
- ²¹In the high- T_c superconductors, there have been some disputes on how to interpret the conductivity spectra below 1.0 eV. Some workers tried to interpret them in terms of the one component model using the frequency dependent scattering rate. Other workers explained them in terms of the two component model which includes a Drude peak in the far-IR region and a mid-IR peak. See D. B. Tanner and T. Timusk, in *Physical Properties of High Temperature Superconductors III*, edited by D. M. Ginsberg (World Scientific, Singapore, 1992), Chap. 5.
- ²²K. Kamarás, S. L. Herr, C. D. Porter, N. Tache, D. B. Tanner, S. Etemad, T. Venkatesan, E. Chase, A. Inam, X. D. Wu, M. S. Hegde, and B. Dutta, *Phys. Rev. Lett.* **64**, 84 (1990).
- ²³W. Zimmermann, E. H. Brandt, M. Bauer, E. Seider, and L. Genzel, *Physica C* **183**, 99 (1991).
- ²⁴The change of $\sigma_1(\omega=12\Delta)/\sigma_1(\omega=4\Delta)$ with the change of $1/\tau$ should result in the corresponding change of $\mathcal{T}(\omega=12\Delta)/\mathcal{T}(\omega=4\Delta)$.
- ²⁵Assuming $1/\tau=250\text{ cm}^{-1}$ and $2\Delta/k_B T_c=4.0$, we could explain the experimental transmission spectra of a BKBO film, measured by Dunmore *et al.* (Ref.4), quite well. We did not have to rely on the Eliashberg equation which was used by Dunmore *et al.*
- ²⁶T. Itoh, K. Kitazawa, and S. Tanaka, *J. Phys. Soc. Jpn.* **53**, 2668 (1984).
- ²⁷B. Batlogg, *Physica B & C* **126**, 275 (1984).
- ²⁸M. Suzuki and T. Murakami, *Solid State Commun.* **53**, 691 (1985).
- ²⁹M. Suzuki, *Jpn. J. Appl. Phys., Part 1* **31**, 3830 (1992).
- ³⁰For material with two types of carriers, suppose that conductivity and mobility of the first carrier (metallic) are larger than those of the second carrier (nonmetallic), i.e., $n_1\mu_1 > n_2\mu_2$ and $\mu_1\mu_2$. Then in the first order, the measurement of Hall effect gives $n_H \approx n_1 + 2(\mu_2/\mu_1)n_2$ and $\mu_H \approx \mu_1 - (n_2/n_1)\mu_2$.
- ³¹K. H. Kim, J. H. Jung, and T. W. Noh, *Phys. Rev. Lett.* **81**, 1517 (1998).
- ³²Due to lattice mismatch between BPBO film and MgO substrate, the first several layers grown on the substrate may have a lower T_c . As stress relieves for the upper layers, bulklike higher T_c could be obtained. For this configuration, the average of $1/\sigma(\omega)$ would be proper.